

Growth and transport property studies of Anthracene - a wide band gap organic semiconductor

J. Rajeev Gandhi¹, and N.Marimuthu²,

1. CCMS National Taiwan Univeristy, Taipei, Taiwan, 106, R.O.C

2. Materials Research Center, Department of Physics, Velammal Engineering College, Chennai. 600066, India.

Abstract

Organic semiconductor investigation and production plays a major role in electronics. The growth of bulk anthracene materials remains one of the most challenging tasks in materials processing. In the present work we propose an efficient and simple synthesis route for anthracene single crystal growth. We have grown anthracene crystals of size $2.7 \times 2.2 \text{ cm}^2$ by slow evaporation technique using Erlenmeyer flask. The size of the grown crystal is considerably bigger than the previously reported crystal sizes. Grown anthracene crystal was subjected to different characterizations such as XRD, UV-visible, FTIR, and dielectric studies. The frequency dependent transport characteristics of the grown Anthracene crystal have been studied in the frequency range of 1KHz to 3MHz.

Keywords: Anthracene crystal, Erlenmeyer flask, Dielectric studies

I INTRODUCTION

Organic semiconductors have some evidences of self-radiation, flexibility, light weight, easy fabrication, and low cost. They have been investigated as organic electroluminescence materials for the applications in organic solar cells, bio sensitizers and display devices such as OLED (Organic Light Emitting Diode), OTFT (Organic Thin Film Transistor), and Wearable Display [1,2]. Anthracene is a tricyclic aromatic hydrocarbon derived from coal tar; melts at 218°C , boils at 354°C , insoluble in water but it is soluble in most organic solvents such as carbon disulfide, alcohols, benzene, chloroform, and hydronaphthalenes. Its molecular structure consists of three benzene like rings joined side by side (the general formula $\text{C}_n\text{H}_{2n-18}$) and its oxidation yields anthraquinone, the parent substance of a large class of dyes and pigments. Anthracene is one of the organic molecular crystals, which exhibits peculiar optical and electronic properties has attracted much attention [3]. Anthracene single crystals were grown by various techniques, such as Bridgman–Stockbarger, the physical vapor transfer, self-seeding vertical Bridgman technique (DRSSVBT) and solution techniques [4–12]. In this paper, high-quality and large-size Anthracene single crystals were grown by a solution technique. The solvent evaporation was controlled by Erlenmeyer Flasks. The grown crystals were subjected to optical and electrical characterizations.

II EXPERIMENTAL DETAILS:

1. Selection of solvents and controlling the solvent evaporation

The solvent selection was done based on the solubility ratio. The solvents such as carbon tetrachloride, acetone, benzene, carbon bisulfide, and carbon dichloride have been tried. Based on solubility ratio carbon bisulfide was chosen as the suitable solvent for this study. The best containers to use are (in the order): centrifuge tube, NMR tube, test tube, round bottom flask, conical flask or Erlenmeyer flask and beaker. In the present study Erlenmeyer flasks are preferred over beakers for recrystallization because the conical shape of an Erlenmeyer flask decreases the amount of solvent lost to evaporation during heating, prevents the formation of a crust around the sides of the glass, and makes it easier to swirl the hot solution while dissolving the solid without splashing it out of the flask as shown in fig1. To have the perfect defect free clear and bulk crystals, we have to control the solvent evaporation. To increase the nucleation rate and produce large crystals we prefer the complete solution is placed in Erlenmeyer flask. The sloping sides of the Erlenmeyer flasks make them the best choice for a crystallization flask, since they reduce the amount of solvent lost to evaporation. Good crystal growth accompanied by expulsions of impurities requires space (depth) in solution. This is achieved by Erlenmeyer flask. Narrow neck allows some refluxing of the solvent. So that the evaporation from the surface is minimized.



Fig1. Erlenmeyer flask for crystallization

2. Crystal growth:

Anthracene crystal was grown by solution method in which the temperature and concentration are important parameters. In solution growth technique there are two ways of controlling the solvent evaporation- slow cooling and slow evaporation. Compared to another techniques it is low cost, need only low temperature and easy to observe the crystal growth process. In our experiment, Anthracene single crystals were grown by slow evaporation of the solvent at room temperature. We have used carbon bisulfide as solvent for the crystal growth experiment.

150ml carbon bisulfide was taken in a glass beaker and 4g of 99.9% pure anthracene(Merck) powder was added to obtain a saturated solution by continues stirring, and then the solution was filtered to remove the insoluble impurities. After filtering, the solution was transferred into the Erlenmeyer flasks and it was sealed using an aluminum foil to avoid deposition of dust on the solution surface. The volatilization rate of solvents were controlled small pores drilled on foil surface.. Since Anthracene solution tends to be oxidized by photo irradiation in the presence of oxygen, the solution was always placed in a dark environment. Crystals were grown from carbon bisulfide by allowing a saturated solution to evaporate slowly at room temperature. In present work well-faceted anthracene crystals of maximum size 2.7x2.2 cm² in area and 0.5 mm thick were grown (fig.2)

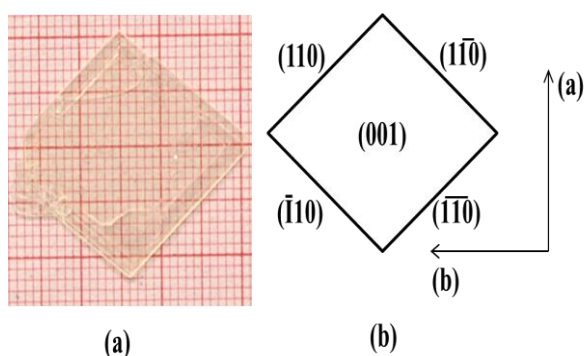


Fig.2. (a) Grown Anthracene single crystal, (b) morphology of grown crystal

The prominent faces of Anthracene single crystals grown from solution are those which correspond to planes with small reticular areas. From crystal morphology diagram shown in Fig, 2(b) it is clear that the basal plane(001) is surrounded by (110), ($\bar{1}10$), ($\bar{1}\bar{1}0$), and ($\bar{1}\bar{1}0$) ($20\bar{1}$) planes. The morphology of the crystals grown from solution is affected by many factors, such as temperature, supersaturation, surface tension, surface energy, and the crystal-solvent interactions on the interface. The surface roughness is mainly determined by temperature, supersaturation, and surface tension [13-16].

III. CHARACTERIZATION

Powder X-ray diffraction studies of the finely crushed anthracene crystalline powder was carried out by Rigaku D/max-A diffractometer fitted with CuK α radiation ($\lambda=1.5406\text{\AA}$) at scan speed 0.01^o/s at room temperature. The

diffracted intensity data was recorded by continues scan in 2 θ / θ mode from 10^o to 70^o. The absorption spectra of grown crystals were studied using Varian Cary 5E UV-visible –NIR spectrometer in the spectral region of 200-2500 nm. In order to identify the organic functional groups, FTIR spectrum was done at room temperature in the range of 400-4500 cm⁻¹. Perkin Elmer FTIR spectrometer was employed to record the spectrum using KBr pellet method. The frequency dependent dielectric constant, dielectric loss and ionic conductivity measurements were carried out at room temperature using Wayne Kerr precision component analyzer (Models WK6440B) in the frequency range 100 kHz–3MHz.

IV. RESULT AND DISCUSSION:

1. X-Ray diffraction

The X-ray powder patterns of the grown crystals were recorded using Bruker D4 X-ray diffractometer. Monochromatic intense X-ray of wave length 1.5406 Å (Cu K α) was used. Fig.3 shows the X-ray diffraction pattern anthracene crystals. The diffraction patterns agreed very well with the data of standard for Anthracene (JCPDS NO: 39-1848).

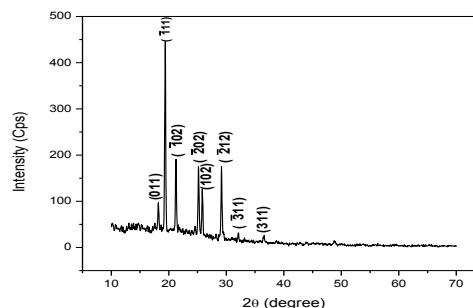


Fig.3. XRD pattern of Anthracene crystals

2. Optical absorption Studies

The optical absorption spectra of grown crystals were studied using Varian Cary 5E UV-visible –NIR spectrometer in the spectral region of 200-2500 nm. UV-visible absorption spectrum of anthracene single crystal shown in fig.4 has four absorption peaks at 323, 339, 357 and 377nm.

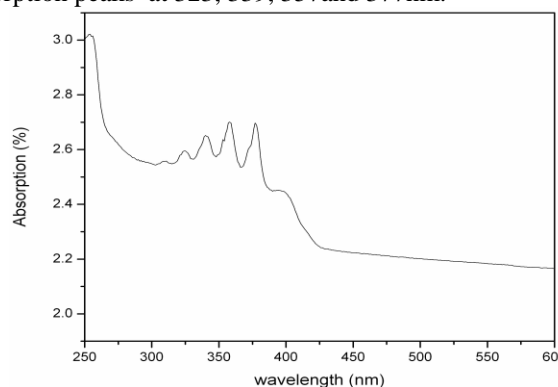


Fig.4. UV absorption spectrum of Anthracene

The study of band gap energy has prominent place in the determination of semiconductor parameters. The absorption coefficient (α) for Anthracene was calculated using the following relation for high photon energies ($h\nu$):

$$\alpha = \frac{A(h\nu - E_g)^{1/2}}{h\nu}$$

Where E_g is optical band gap of the Anthracene crystal and A is constant. Energy gap can be determined by optical absorption method. From the plot of $(\alpha h\nu)^2$ Vs $(h\nu)$ shown in fig.5 the band gap was calculated and found to be 2.42 eV.

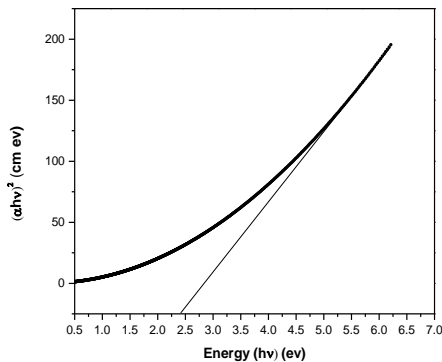


Fig.5. Plot of variation of spectrum of $(\alpha h\nu)^2$ Vs $(h\nu)$

3. FTIR-Analysis

The grown crystal was subjected to Fourier Transform Infra-Red (FTIR) analysis in order to determine the functional groups present in the crystal. The Anthracene vibrational mode are recorded with the help of Bruker IFS 66 V spectrophotometer in the range of 4500-450 cm^{-1} by KBr pellet method. These vibrational modes are shown in Fig.6.

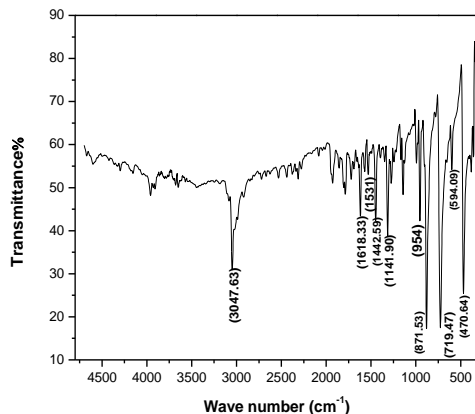


Fig.6. FTIR spectrum of Anthracene Crystals

A very sharp peak at 3047.63 cm^{-1} is the characteristic peak due to C-H stretch vibration. The sharpness of the peak elucidates that the hydrogen atoms in the anthracene ring are not exerting any bonding interaction with molecules. The skeletal vibrations of the ring could be assigned to peaks 1618.33 , 1531 and 1442.90 cm^{-1} . The peak at 719.47 cm^{-1} confirms the presence of four adjacent hydrogen atoms [6].

4 Dielectric measurement:

a) Dielectric constant

The dielectric behaviors of Anthracene crystals were studied at different frequency and temperature. The range of temperature is fixed from RT to 373k. In this study, the parallel plate capacitor was formed by two copper electrodes and the single crystal which is coated by silver paste on opposite side is placed between the electrodes. This arrangement made a perfect capacitor. The dielectric constant was calculated by the following relation.

$$\epsilon_r = \frac{cd}{A\epsilon_0}$$

Here,

c- Capacitance of the sample

d- Sample thickness

A- Surface area of the sample and ϵ_0 is permittivity of free space ($8.854 \times 10^{-12} \text{ F/m}$).

Fig7. shows frequency dependent dielectric constant of Anthracene crystals at selected temperatures.

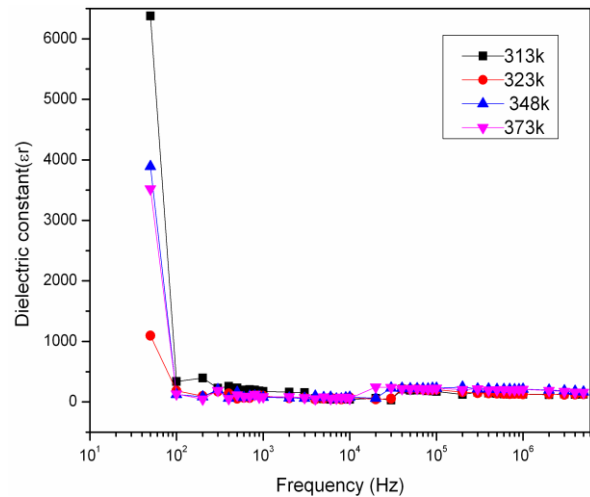


Fig. 7. Dielectric constant vs frequency

All polar molecules have high dielectric constant. Anthracene which has very low polar molecules have low dielectric constant. From figure 7 it is observed that dielectric constant of Anthracene is high at low frequency which is due to the contribution of ionic, electronic, dipolar, orientation and space charge polarization [17]. Space charge polarization is dominant at low frequencies. But space charge polarization diminishes as the frequency increases and the other polarization mechanisms having large relaxation time cease to respond to the applied electric field. Hence, the contribution from other polarization becomes low or even absent. At high frequencies, only electronic polarization with large relaxation

time exists and all other polarizations cease [18]. Hence the net dielectric constant decreases as frequency increases. It is also observed that dielectric constant decreases with increasing temperature.

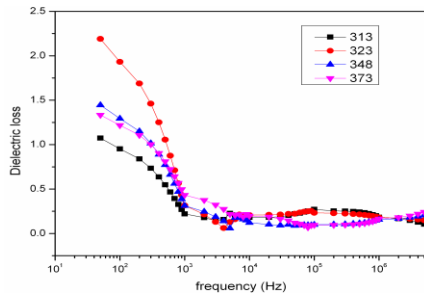


Fig 7.a Dielectric loss Vs Frequency

b) Dielectric loss

The loss tangent ($\tan \delta$) is the ratio of the loss factor to the relative permittivity, and is a measure of the ratio of the electric energy loss to the energy stored in a periodic field. Fig7 shows the variation of tangent loss with frequency for anthracene crystal in the temperature range 308 -373 K. It is observed that tangent loss ($\tan\delta$) for all the samples attains higher value at low frequency and decreases with increasing frequency, illustrating the relaxation process. The observed higher dielectric loss at lower frequency may be due to an accumulation of free charges.

5 Ac conductivity studies

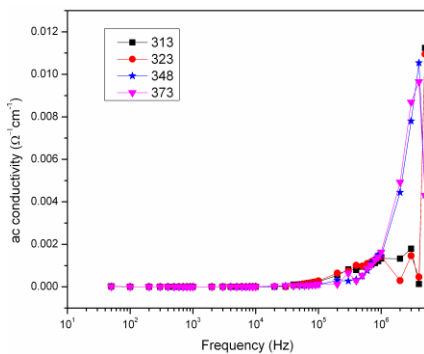


Fig 8. Frequency Vs ac conductivity

The conductivity representation is a most prominent representation to relate the macroscopic measurement to the microscopic movement of the ions.[19]. Fig.8 shows the plot of electrical conductivity and frequency for various temperatures (313k, 323k, 348k, and 373k). In range of experimental frequencies (1 KHz -3 MHz) the conductivity follows the Jonscher's power law relation $\sigma=A\omega^s$, where ω is the angular frequency, A is constant and the exponent s is a frequency dependent parameter having values less than unity. AC conductivity was calculated using the formula $\sigma=\omega\epsilon_0\epsilon_r\tan\delta$, where ω is angular frequency ($\omega=2\pi f$); $\tan\delta$ is dielectric loss and ϵ_0 and ϵ_r are the permittivity of free space

and dielectric constant of the sample respectively. From fig.8 it is also observed that as the temperature increases, ac conductivity increases which may be due to increases in the drift mobility of thermally activated electrons.[20] Hence the conductivity increases with frequency and temperature in Anthracene. However an anomaly was observed, in the higher frequency region at lower temperature (313K) Anthracene has higher conductivity which may be an experimental error.

V. CONCLUSION

Large-size and good quality Anthracene single crystals were grown by a slow evaporation technique using Erlenmeyer flask. The grown crystals were subjected to different characterizations, such as XRD, UV, FTIR, dielectric constant and AC conductivity. The absorption peaks and hence energy band gap were found by from UV absorption spectrum. The band gap value of anthracene was found to be 2.4eV. From the FTIR spectrum the C–H stretch, skeletal vibrations and presence of four adjacent hydrogen atoms are confirmed. Dielectric measurement shows that the value of dielectric constant decreases with increasing the frequency and the A.C conductivity increased with increasing the frequency.

REFERENCES

- 1.R.W.I. de Boer, M.E. Gershenson, A.F. Morpurgo and V. Podzorov, Phys. Status Solidi (A) 201 (2004) 1302–1331.
- 2.V.C. Sundar, J. Zaumseil, V. Podzorov, E. Menard, R.L. Willett, T. Someya, M.E. Gershenson and J.A. Rogers, Science 303 (2004) 1644–1646.
- 3.A.N. Aleshina, J.Y. Lee, S.W. Chu, J.S. Kim and Y.W. Park, Appl. Phys. Lett. 84 (2004) 5383–5385.
- 4.J. Niemax and J. Pflaum, Appl. Phys. Lett. 87 (2005) 241921.
- 5.A. Arulchakkaravarthi, C.K. Laksmanaperumal, P. Santhanaraghavan, P. Jayavel, R. Selvan, K. Sivaji, R. Gopalakrishnan and P. Ramasamy, Mater. Sci. Eng. B 95 (2002) 236–241.
- 6.A. Arulchakkaravarthi, C.K. Laksmanaperumal, P. Santhanaraghavan, K. Sivaji, R. Kumar, S. Muralithar and P. Ramasamy, J. Cryst. Growth 246 (2002) 85–89.
- 7.S. Jo, H. Yoshikawa, A. Fujii and M. Takenaga, Jpn. J. Appl. Phys. 44 (2005) 4187–4188.
- 8.S. Jo, H. Yoshikawa, A. Fujii and M. Takenaga, Surf. Sci. 592 (2005) 37–41.
- 9.S. Jo, H. Yoshikawa, A. Fujii and M. Takenaga, Appl. Surf. Sci. 252 (2006) 3514–3519.
- 10.M. Pope and H. Kallmann, Rev. Sci. Instrum. 29 (1958) 993–994.

- 11.V.V. Podolinsky and V.G. Drykin, J. Cryst. Growth 62 (1983) 532–538.
- 12.G. Madhurambal and P.A. Srinivasan, Cryst. Res. Technol. 41 (2006) 231–235.
- 13.Pengqiang Zhang, Jour. of Cry. Gro. 311 (2009) 4708–4713.
- 14.Sadaharu Jo et al, Applied Surface science 252(2006)3514-3519
- 15.P.M.Robinson and H.G Scott, Jl.of Crystal Growth1(1967)187-194
- 16.H.P. Li, D.Q. Zhang, L. Duan, G.F. Dong, L.D. Wang, Y. Qiu., Jpn. J. Appl. Phys. 46 (2007) 7789–7792.
- 17.A. Ashok, T. Somaiah, D. Ravinder, C. Venkateshwarlu, C. Reddy, K. Rao, M. Prasad,. World J. Condens. Matter Phys. 2, 257–266 (2012)
- 18K. TamizhSelvi, K. Alamelumangai, M. Priya, M. Rathnakumari, P. Suresh Kumar, Suresh Sagadevan “J Mater Sci: Mater Electron.27, 6457–6463 (2016)
- 19.Nidhi Sinha ,.Manoj K.Gupta,Neeti Goel and Binay Kumar, Physics, B406(2011)3206-3209
- 20.Siby Kurien, Shajo Sebastian, Jose Mathew and K.C. George, Indian. J. Pur. & appl.phys. 42 (2004) 926-933.